COMPARISON OF DEPOLARIZATION RATIO MEASUREMENTS WITH MICRO-PULSE LIDAR AND A LINEAR POLARIZATION LIDAR IN LANZHOU, CHINA

Zhongwei Huang[1, 2], Nobuo Sugimoto[3], Jianping Huang[1], Tadahiro Hayasaka[2], Tomoaki Nishizawa[3], Jianrong Bi[1], and Ichiro Matsui[3]

[1] *Key Laboratory for Semi-Arid Climate Change of the Ministry of Education, College of Atmospheric Sciences, Lanzhou University, Lanzhou, China.* *Email: huangzhongwei@lzu.edu.cn*
[2] *Center for Atmospheric and Oceanic Studies, Tohoku University, Sendai, Japan*
[3] *Atmospheric Environment Division, National Institutes for Environmental Studies, Tsukuba, Japan*

ABSTRACT

Measurements of mineral dust and cirrus cloud with a Micro-Pulse Lidar (MPL4) and a linear polarization lidar were compared at the Semi-Arid Climate and Environment Observatory of Lanzhou University (SACOL) site in Lanzhou, China. The linear depolarization ratio converted from the MPL depolarization ratio agreed with that measured with the linear polarization lidar within 10%. However, slight systematic differences were seen in cirrus cloud and mineral dust measurements in different senses. Non-random orientation of ice particles in cirrus cloud may be the causes of the differences, but the reason for the mineral dust particles is not known. The difference does not significantly affect the total lidar signal power of MPL4, and the attenuated backscattering coefficients from the two lidars agreed reasonably.

1. INTRODUCTION

The understanding of the direct, indirect, and semi-direct effects of mineral dust is still low compared to other atmospheric aerosols although dust-related effects are potentially large [1, 2]. The difficulty in studying the mineral dust aerosol is due to the heterogeneity in both space and time of their concentrations and properties, and to the complexity of their compositions that evolve during their transport including possible interactions with other aerosols and clouds [3, 4]. Especially, the vertical distribution of mineral dust in the atmosphere is a key element in estimating its effect on radiative forcing and associated climatic impacts [5, 6, 7, 8], which must be assessed over the world.

We plan to build a lidar observation network for detecting the optical properties of mineral dust over Northern China, which is one of the largest dust sources and seriously affected by dust events due to several dust deserts there (e.g., Takalimakan desert and Gobi desert). Each observation site of the network will employ a ground-based Mie-scattering polarization lidar system and a sun photometer (or sky radiometer). Some solar spectral radiometers and sampling meters perform necessary dust monitoring tasks at some basic sites. Space-borne measurements (e.g., CALIPSO and OMI) over the region also provide important information about mineral dust. Furthermore, that cooperating with other developed networks (e.g. AERONET, SKYNET and AD-NET) for investigating aerosol climatic effects will help us better observe long-range transport mechanisms of dust storms and air pollution. Therefore, vertical and horizontal distributions of optical properties of mineral dust both in space and time in the atmosphere and other associated environmental problems and the mechanism of dust emission and long-distance transport, over Northern China even to East Asia, will be directly obtained from the network observation. Simulations of microphysical and chemical properties of mineral dust and its radiative forcing will benefit from the results of the lidar network observation by some related models (i.e., Fu-Liou radiation model and CFORS). In other word, our network observation will help us better understand the impact of mineral dust on the climate and climate change, and early warning of dust events and air pollution in East Asia.

However, one of the difficulties we encountered was that there are different types of lidar systems for detecting vertical distributions of atmospheric aerosols and clouds in the network. Therefore, it is very important to use intercomparison measurements to check the performance and reliability of individual lidar systems. In order to determine the precision of each lidar system, a MPL4 and a linear polarization lidar were located close together and probed nearly the same volume of aerosol and clouds in the atmosphere.

In this paper, comparisons of instruments and observation results between NIES lidar and MPL4 were studied using lidar measurements at SACOL site [9] in Lanzhou, China, beginning in November 2009. The introduction of two different types of lidar systems and the method will be described in section 2

and intercomparison results will be shown and discussed in section 3.

2. MEASUREMENTS AND METHOD

The polarization lidar observations were performed by two different Mie-scattering lidar systems at SACOL site. One was developed by NIES in Japan for continuous network observations. It employs a flash-lamp-pumped, second-harmonic Nd: YAG laser and a receiver telescope with a diameter of 20cm. The transmitted laser (532nm) is linearly polarized, and two polarization components of the scattered light were detected with two photomultiplier tubes [10]. Five-minute measurements are taken automatically every 15min typically in long-term observations. The other is a polarized MPL4 that is an eye-safe, compact and maintenance-free lidar system originally developed by Spinhirne [11]. The MPL4 uses an Nd: YLF pulsed laser diode, operating at a wavelength of 527 nm. The continual aerosol and cloud measurements are acquired with a 30-m range resolution and a 1-min time average. MPL4 has a depolarization ratio measurement capability using an actively controlled liquid crystal retarder to switch between the two different modes. MPL measures the cross polar signal with a linearly polarized transmitted beam and the co-polar signal with a circularly polarized beam [12]. The depolarization ratio obtained is so-called MPL depolarization ratio. The MPL depolarization ratio is defined by

$$\delta_{MPL} = \frac{\left|\vec{P}_{\perp}(0)\right|}{\left|\vec{P}_{\perp}(\pi/2)\right|}$$

Using the general form of the Mueller matrix for backscattering [13],

$$F = \begin{pmatrix} a_1 & b_1 & b_3 & b_5 \\ b1 & a_2 & b_4 & b_6 \\ -b_3 & -b_4 & a_3 & b_2 \\ b_3 & b_6 & -b_2 & a_4 \end{pmatrix}$$

The linear depolarization ratio, the circular polarization ratio, and the MPL depolarization ratio can be written as follows.

$$\delta_{MPL} = \frac{\left|\vec{P}_{\perp}(0)\right|}{\left|\vec{P}_{\perp}(\pi/2)\right|} = \frac{a_1 + a_3}{a_1 - a_4}$$

$$\delta_{linear} = \frac{\left|\vec{P}_{\perp}(0)\right|}{\left|\vec{P}_{\parallel}(0)\right|} = \frac{a_1 + a_3}{a_1 + 2b_3 - a_3}$$

$$\delta_{circ} = \frac{\left|\vec{P}_{\parallel}(\pi/2)\right|}{\left|\vec{P}_{\perp}(\pi/2)\right|} = \frac{a_1 + 2b_5 + a_4}{a_1 - a_4}$$

From these equations, the following relationship is found between δ_{linear} and δ_{MPL}.

$$\delta_{linear} = \delta_{MPL} / (\delta_{MPL} + c)$$

Where $c = (2b_3 - 2a_3)/(a_1 - a_4)$.
The total lidar signal power and attenuated backscattering coefficient for MPL can be then written as,

$$\left|\vec{P}\right| = c\left|\vec{P}_{\perp}(\pi/2)\right| + 2\left|\vec{P}_{\perp}(0)\right|$$

$$\beta_{att} = \left|\vec{P}\right| / C_{lidar}$$

Here C_{lidar} is the system constant of lidar. If the particles are randomly oriented, b_3=0, a_2=-a_3 and a_4=a_1-2a_2, and consequently c=1. However, c can differ from 1, in general.

In order to study the relationships between the linear depolarization ratio and the MPL depolarization ratio for different types of scatterers, three cases are considered (namely, cirrus cloud, mineral dust and background aerosol). The selection criterion for each case is as follows: a) Cirrus cloud: the data above 3 km having the attenuated backscattering coefficients measured with NIES lidar are larger than 0.2 (10^{-5}/m/sr) and smaller than 10.0 (10^{-5}/m/sr); b) Mineral dust aerosol: all particles below 3km from Dec. 24 to 31, 2009 and Jan. 19 to 29, 2010 where high depolarization ratios were observed c) Background aerosol: except for the above two cases, all remaining particles are considered as background aerosol.

3. RESULTS AND DISCUSSION

Depolarization lidar measurements from two different types of lidar systems at SACOL site in Lanzhou, China from Nov. 24, 2009 to Jan. 29, 2010 are used in this study (Fig. 1). Attenuated backscattering coefficients from NIES lidar observations were shown as Fig. 1a. Fig. 1b and 1c show different depolarization ratios observed by

NIES lidar and MPL lidar, respectively. Two wintertime dust events were both observed by two-lidar systems. We can see that mineral dust aerosols and cirrus cloud both exhibited high depolarization ratios.

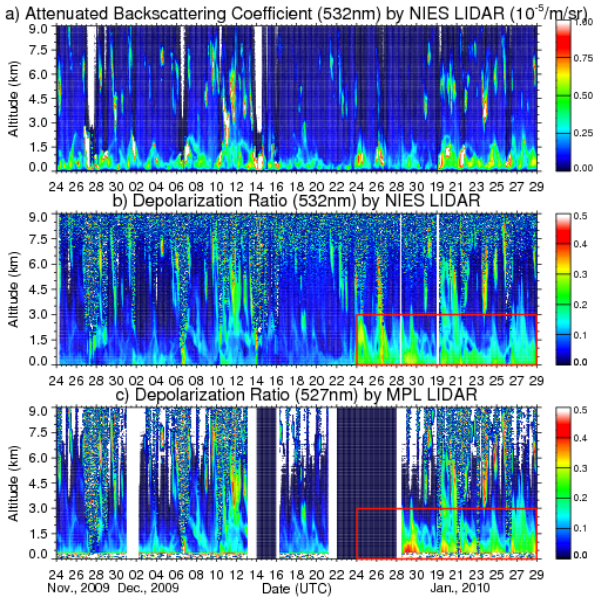

Fig. 1. Lidar observations of a) attenuated backscattering coefficients from NIES lidar, b) linear depolarization ratio by NIES lidar and c) MPL depolarization ratio at SACOL for Nov. 24, 2009 to Jan. 29, 2010. Red boxes denote the regions of dust aerosol.

The relationships between linear depolarization ratio observed by NIES lidar and MPL depolarization ratio for different types of particles were shown in Fig. 2. The depolarization ratio of cirrus cloud is very high (mostly greater than 0.3) and the relationship between two different polarized observations is decentralized and not obvious. However, it is more centralized for background aerosol and especially for dust aerosol. One of the reasons for this phenomenon may be that cirrus cloud have much more multi-scattering effects than the other two types. For different types of particles, c equals to 0.913, 1.0 and 1.085 for cirrus cloud, background aerosol and mineral dust, respectively. Our results agree well with the Connor's results for background aerosol but not for mineral dust aerosol and cirrus cloud.

MPL depolarization ratios of cirrus cloud and mineral dust aerosol are converted to linear depolarization ratio by assuming c=1 and then compared with those from NIES lidar observations (Fig. 3). Orange and blue colors represent dust aerosol and cirrus cloud respectively. We can see that linear depolarization ratio of cirrus cloud exceeds those of dust aerosol in winter. The differences are quite obvious, although reasonable, for cirrus cloud and mineral dust. One of the reasons for our results is that ice crystals have a non-random orientation, but for mineral dust is not known.

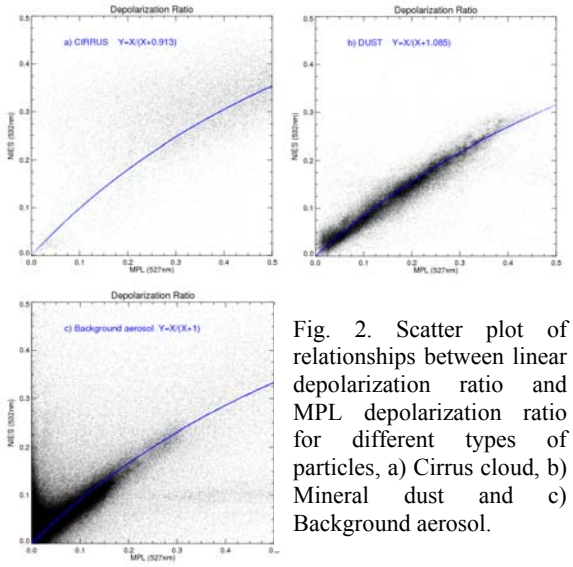

Fig. 2. Scatter plot of relationships between linear depolarization ratio and MPL depolarization ratio for different types of particles, a) Cirrus cloud, b) Mineral dust and c) Background aerosol.

The total lidar signal power for MPL were used to obtain attenuated backscattering coefficients and compared with those from NIES lidar indicated reasonable agreement between them.

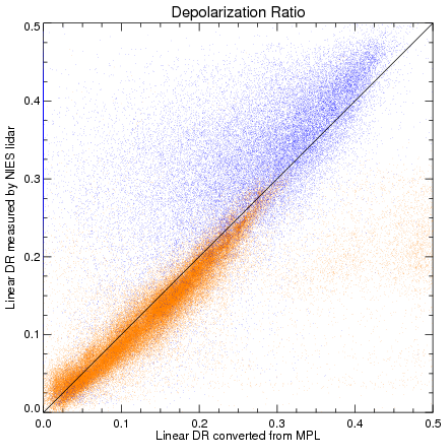

Fig. 3. Comparisons between linear depolarization ratios measured by NIES lidar and converted from MPL polarization observations using Connor's relationship. Orange and blue colors denote dust aerosol and cirrus cloud respectively.

4. CONCLUSION

The linear polarized NIES lidar observations were compared directly with the polarized MPL lidar observations. The relationships between linear

depolarization ratio and MPL depolarization ratio depend on four elements (a1, a3, a4, and b3) of the backscattering Mueller matrix. Non-random orientation of ice particles in cirrus cloud may be the causes of the difference but for mineral dust it is still not known. The difference does not significantly affect the total lidar signal power of MPL, and the attenuated backscattering coefficients from the two lidars agreed reasonably. Further measurements results will be discussed at the conference.

5. ACKNOWLEDGEMENT

This research is supported by National Science Foundation of China under Grants No. 40725015,and 40633017, and by the Grant-in-Aid for Scientific Research on Innovative Area under the Grant No. 4003 from the Ministry of Education, Culture, Sports, Science and Technology of Japan. Zhongwei Huang is a visiting PH.D. student supported by the government scholarship from China Scholarship Council (CSC). We would also like to thank Dr. Wenbo Sun for his useful comments.

6. REFERENCES

[1]. Intergovernmental Panel on Climate Change (2001), Climate Change 2001: The Science of Climate Change-Technical Summary of the Working Group I Report, World Meteorol. Organ., Geneva, Switzerland.

[2]. Helmert, J., B. Heinold, I. Tegen, O. Hellmuth, and M. Wendisch, 2007: On the direct and semidirect effects of Saharan dust over Europe: A modeling study, J. Geophys. Res., 112, D13208, doi: 10.1029/2006JD007444.

[3]. Chester, R., 1986: The marine mineral aerosol, in The Role of Air-Sea Exchange in Geochemical Cycling, NATO ASI Ser., Ser. C, vol. 185, edited by P. Buat-Me´nard, pp. 443 – 471, Springer, New York.

[4]. Guieu, C., M. D., Loye-Pilot, C. Ridame, and C. Thomas, 2002: Chemical characterization of the Saharan dust end-member: Some biogeochemical implications for the western Mediterranean Sea, J. Geophys. Res., 107(D15), 4258, doi: 10.1029/2001JD000582.

[5]. Claquin, T., M. Schulz, Y. J. Balkanski, and et al., 1998: Uncertainties in assessing radiative forcing by mineral dust, Tellus, 50(B), 491–505.

[6]. Forster, P., V. Ramaswamy, P. Artaxo, and et al., 2007: Changes in atmospheric constituents and in radiative forcing. In: Climate Change 2007: The Physical Science Basis, Working Group I to the Fourth Assessment Report of the Intergovernmental Panel on Climate Change, United Kingdom and New York: Cambridge University Press, Cambridge, 2007, 129-234.

[7]. Huang, J., P. Minnis, B. Chen, Z. Huang, Z. Liu, Q. Zhao, Y. Yi, and J. K. Ayers, 2008: Long-range transport and vertical structure of Asian dust from CALIPSO and surface measurements during PACDEX, J. Geophys. Res., 113, D23212, doi: 10.1029/2008JD010620.

[8]. Huang J., Q. Fu, J. Su, Q. Tang, P. Minnis, Y. Hu, Y. Yi, and Q. Zhao, 2009: Taklimakan dust aerosol radiative heating derived from CALIPSO observations using the Fu-Liou radiation model with CERES constraints, Atmos. Chem. Phys., 9, 4011–4021.

[9]. Huang, J., et al., 2008: An overview of the semi-arid climate and environment research observatory over the Loess Plateau. Adv. Atmos. Sci., 25(6), 906–921, doi: 10.1007/s00376-008-0906-7.

[10]. Sugimoto, N., I. Matsui, A. Shimizu, T. Nishizawa, Y. Hara, C. Xie, I. Uno, K. Yumimoto, Z. Wang, S-C. Yoon, “Lidar Network Observations of Troposheric Aerosols”, SPIE Vol. 7153, 2008 doi: 10.1117/12.806540.

[11]. Spinhirne, J. D., 1993: Micro pulse lidar, IEEE Trans. Geosci. Remote Sens. 31, 48–55.

[12]. Connor J. F., A. Mendoza, Y. Zheng, and S. Mathur, 2007: Novel polarization-sensitive micropulse lidar measurement technique, OPTICS EXPRESS, 15(6), 2785-2790.

[13]. Hulst, H. C. Van De, 1981: Light Scattering by Small Particles, Dover, New York.